Inorganic Chemistry

Article

pubs.acs.org/IC

Synthesis, Structure, and Magnetic Properties of Regular Alternating μ-bpm/di-μ-X Copper(II) Chains (bpm = 2,2′-bipyrimidine; X = OH, F)

Nadia Marino,[†,∥] Donatella Armentano,[†] Giovanni De Munno,*[,†] Joan Cano,[‡,§] Francesc Lloret,[‡] and Miguel Julve*[,‡]

[†]Centro di Eccellenza CEMIF.CAL, Dipartimento di Chimica, Università della Calabria, via P. Bucci 14/c, 87030 Arcavacata di Rende, Cosenza, Italy

[‡]Departament de Química Inorgànica/Instituto de Ciencia Molecular (ICMol), Universitat de València, C/Catedrático José Beltrán 2, 46980 Paterna, València, Spain

[§]Fundació General de la Universitat de València (FGUV), 46980 Paterna, València, Spain

Supporting Information

ABSTRACT: The preparation and X-ray crystal structure of four 2,2′-bipyrimidine (bpm)-containing copper(II) complexes of formula $\{[Cu_2(\mu\text{-bpm})(H_2O)_4(\mu\text{-OH})_2][Mn(H_2O)_6](SO_4)_2\}_n$ (**1**), $\{[Cu_2(\mu\text{-bpm})(H_2O)_4(\mu\text{-OH})_2]SiF_6\}_n$ (**2**), $\{Cu_2(\mu\text{-bpm})(H_2O)_2(\mu\text{-F})_2F_2\}_n$ (**3**), and $[Cu(bpm)(H_2O)_2F(NO_3)][Cu(bpm)(H_2O)_3F]NO_3\cdot 2H_2O$ (**4**) are reported. The structures of **1**−**3** consist of chains of copper(II) ions with regular alternation of bis-bidentate bpm and di-μ-hydroxo (**1** and **2**) or di-μ-fluoro (**3**) groups, the electroneutrality being achieved by either hexaaqua manganese(II) cations plus uncoordinated sulfate anions (**1**), uncoordinated hexafluorosilicate anions (**2**), or terminally bound fluoride ligands (**3**). Each copper(II) ion in **1**−**4** is six-coordinated in elongated octahedral surroundings. **1** and **2** show identical, linear chain motifs with two bpm-nitrogen atoms and two hydroxo groups building the equatorial plane at each copper(II) ion and the axial position being filled by water molecules. In the case of **3**, the axial sites at the copper atom are occupied by a bpm-nitrogen atom and a bis-monodentate fluoride anion, producing a "step-like" chain motif. The values of the angle at the hydroxo and fluoro bridges are 94.11(6) (**1**), 94.75(4) (**2**), and 101.43(4)° (**3**). In each case, the copper−copper separation through the bis-bidentate bpm [5.428(1) (**1**), 5.449(1) (**2**), and 5.9250(4) Å (**3**)] is considerably longer than that through the di-μ-hydroxo [2.8320(4) (**1**) and 2.824(1) Å (**2**)] or di-μ-fluoro [3.3027(4) Å (**3**)] bridges. Compound **4** is a mononuclear species whose structure is made up of neutral $[Cu(bpm)(H_2O)_2F(NO_3)]$ units, $[Cu(bpm)(H_2O)_3F]^+$ cations, uncoordinated nitrate anions, and crystallization water molecules, giving rise to a *pseudo*-helical, one-dimensional (1D) supramolecular motif. The magnetic properties of **1**−**3** have been investigated in the temperature range 1.9−300 K. Relatively large, alternating antiferro- [$J = -149$ (**1**) and -141 cm^{-1} (**2**) across bis-bidentate bpm] and ferromagnetic [$\alpha J = +194$ (**1**) and $+176$ cm^{-1} (**2**) through the dihydroxo bridges] interactions occur in **1** and **2** [the Hamiltonian being defined as $H = -J\sum_{i=1}^{n/2}(S_{2i}\cdot S_{2i-1} - \alpha S_{2i}\cdot S_{2i+1})$]. These values compare well with those previously reported for parent examples. Two weak intrachain antiferromagnetic interactions [$J = -0.30$ and $\alpha J = -8.1$ cm^{-1} across bpm and the di-μ-fluoro bridges, respectively] whose values were substantiated by density functional theory (DFT)-type calculations occur in **3**.

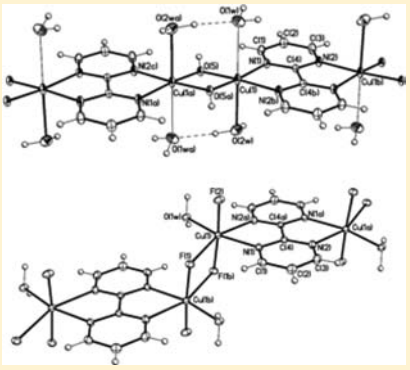

INTRODUCTION

Molecule-based magnetic materials continue to draw considerable attentions for their relevance in the understanding of magneto-structural correlations as well as in the development of new functional systems. One-, two- and three-dimensional (nD, n = 1−3) compounds have been extensively studied in the past not only because of their aesthetic architectures but especially because of the magnetic properties that they exhibit.[1−6] In this area, ordered systems containing different bridging moieties deserve particular attention because alternating magnetic couplings differing in sign and magnitude can occur, depending on the nature and geometry of the ligands.[7−9] In that respect, homometallic 1D compounds with two alternating intrachain antiferromagnetic interactions (J_i and J_{i+1}) are well-known,[7,8] while chains with alternating J_i and J_{i+1} of different sign are still fairly uncommon.[9−12]

Ligands such as cyanide, azide, cyanate, thiocyanate, hydroxide, oxalate, and 2,2′-bipyrimidine (bpm) have been extensively used in magneto-structural studies because of their remarkable ability in mediating magnetic interactions between paramagnetic centers bridged by them and also because of the intriguing magnetic networks that they can originate when adopting different coordination modes in the same structure or when two of them coexist in the corresponding mixed-ligand systems.[11,13−17] In the present contribution, we particularly concentrate on mixed-ligand

Received: January 9, 2012
Published: March 19, 2012

dx.doi.org/10.1021/ic202740b | Inorg. Chem. 2012, 51, 4323−4334

1D complexes of Cu(II) comprising a bpm-bridged dimetallic core.

Focusing on bpm and hydroxide as bridges in copper(II) complexes, whereas the former is able to mediate relatively large antiferromagnetic interactions when adopting the bis-bidentate coordination mode,[11,13−19] the latter one is a ferromagnetic coupler for values of the angle at bridgehead hydroxo-oxygen atom (θ) $\leq$ 97.5° (case of accidental orthogonality between the interacting magnetic orbitals).[20] In the literature, structural data can be found regarding three copper(II) chains with regular alternating di-μ-hydroxo and bis-bidentate bpm bridges and corresponding alternating intrachain ferro-antiferromagnetic couplings, all of which contain nitrate as the counterion.[11a,b] A first magnetic report on a complex of the same family with perchlorate counterion was reported by Hatfield et al. in the early 1990s.[11c]

Multidimensional systems containing M(II) cations (M = Mn, Fe, Co, or Cu) with bridging bpm and pseudohalide anions (X^-) such as N_3^-, NCO^-, or NCS^- have been characterized and magneto-structurally investigated.[14,15a,c,16] In these cases the magnetic coupling through X is usually antiferromagnetic when X exhibits the *end-to-end* (EE) coordination mode or ferromagnetic through the *end-on* (EO) bridging mode. With the azide anion, in particular, 2D honeycomb compounds of general formula $\{[M_2(bpm)(N_3)_4]\}_n$ [M = Mn(II) Fe(II), Co(II)][14b−d] could be obtained showing alternation of antiferro- and ferromagnetic coupling through the bis-bidentate bpm and the EE-azide bridges, respectively. In the Cu(II) 2D complexes of formula $\{Cu_2(\mu\text{-bpm})(N_3)_4\}_n$[14a] and $\{Cu_2(bpm)(NCO)_4\}_n$,[15a] however, each featuring both EE and EO pseudohalide bridges, no ferromagnetic coupling is observed through the EE moiety because of an axial−equatorial asymmetric geometry of the bridge (not in-plane exchange pathway).

By combining bpm with other potentially suitable ions for the construction of alternating magnetic systems, that is, chloride and bromide, asymmetric halide bridges have been observed, again, in the Cu(II) complexes $[Cu_2(bpm)Cl_4]_n$ and $[Cu_2(\mu\text{-bpm})Br_4]_n$,[18a,b] which do not exhibit a linear motif but a 2D honeycomb network similar to that found in the Mn(II), Fe(II), and Co(II) examples with bpm/azide mentioned above.[14b−d] It thus appears hydroxo groups are the most appropriate ligands for the propagation of a bpm-bridged dicopper(II) unit into chains with intrachain "ferro-antiferromagnetic" couplings.

Although such systems have been proven to be quite elusive, we recently came up with unconventional synthetic strategies that afforded two new compounds of this type. As part of this work, we also reconsidered the possibility of utilizing fluoride anions to create a similar alternating system. As far as we know, no examples of fluoro-bpm mixed-ligands polynuclear systems have been reported to date.

Herein, we present the preparation, structural characterization, and magnetic study of three novel copper(II) chains of formula $\{[Cu_2(\mu\text{-bpm})(H_2O)_4(\mu\text{-OH})_2][Mn(H_2O)_6](SO_4)_2\}_n$ (**1**), $\{[Cu_2(\mu\text{-bpm})(H_2O)_4(\mu\text{-OH})_2]SiF_6\}_n$ (**2**), and $[Cu_2(\mu\text{-bpm})(H_2O)_2(\mu\text{-F})_2F_2]_n$ (**3**) exhibiting alternating μ-bpm and di-μ-hydroxo (**1** and **2**) or di-μ-fluoro (**3**) bridges. The crystal structure of the mononuclear complex $[Cu(bpm)(H_2O)_2F(NO_3)][Cu(bpm)(H_2O)_3F]NO_3\cdot 2H_2O$ (**4**), which cocrystallizes with **3**, is also included. Density functional theory (DFT) type calculations have been performed on complex **3** to support the structure−function correlation study.

EXPERIMENTAL SECTION

Materials and Methods. All chemicals were purchased from commercial sources and used as received without further purification. Infrared spectra were recorded on a PerkinElmer 1750 FT-IR spectrometer as KBr pellets in the 4000−400 cm^{-1} region. The relative intensity of reported signals are defined as s = strong, br = broad, sh = sharp, m = medium, and w = weak. Elemental analysis (C, H, N) were performed by the Microanalytical Service of the Università della Calabria.

Synthesis of $\{[Cu_2(\mu\text{-bpm})(H_2O)_4(\mu\text{-OH})_2][Mn(H_2O)_6](SO_4)_2\}_n$ ***(1)***. Pale blue hexagonal prisms of compound **1** were obtained by slow evaporation of an aqueous solution (20 mL) containing $CuSO_4\cdot 5H_2O$ (1 mmol), $MnSO_4\cdot H_2O$ (1 mmol), and bpm (0.5 mmol). The pH of the mother liquor was brought to 6.5−7.0 with 1 M NaOH. Yield: about 80%. Anal. data for **1** ($C_8H_{28}Cu_2MnN_4O_{20}S_2$, MW = 373.24) Calcd: C, 12.87, H, 3.78, N, 7.51%. Found: C, 12.95, H, 4.02, N, 7.72%. FTIR (KBr pellet/cm^{-1}): 3200br, 1662w, 1596sh, 1427s, 1232sh, 1088s, 1068s, 983sh, 710w, 692sh cm^{-1}.

Synthesis of $[Cu_2(\mu\text{-bpm})(H_2O)_4(\mu\text{-OH})_2]SiF_6\}_n$ ***(2)***. Royal blue prismatic crystals of **2** were obtained by slow diffusion in an H-shaped tube at room temperature of an aqueous solution of $Cu(NO_3)_2\cdot 3H_2O$ (0.15 mmol) and bpm (0.15 mmol) into an aqueous solution containing NaF (0.4 mmol). X-ray quality crystals were obtained within two weeks. Yield: about 50%. Anal. data for **2** ($C_8H_{16}Cu_2F_6N_4O_6Si$, MW = 266.71) Calcd: C, 18.01, H, 3.02, N, 10.50%. Found: C, 18.25, H, 2.94, N, 10.75%. FTIR (KBr pellet/cm^{-1}): 3490sh, 3104w, 1667w, 1593s/sh, 1424s/sh, 1232sh, 1043sh, 958s, 713s, 686s cm^{-1}.

Synthesis of $[Cu_2(\mu\text{-bpm})(H_2O)_2(\mu\text{-F})_2F_2]_n$ ***(3)*** *and* $[Cu(bpm)(H_2O)_2F(NO_3)][Cu(bpm)(H_2O)_3F]NO_3\cdot 2H_2O$ ***(4)***. Pale blue-green cubes of compound **3** (main product, yield ca. 50%) and blue parallelepiped-shaped crystals of **4** (a few crystals) were obtained by slow evaporation of an ethanolic solution (20 mL) containing $Cu(NO_3)_2\cdot 3H_2O$ (1 mmol), *n*-Bu_4NF (4 mmol), and bpm (2 mmol). The crystals were filtered and separated by hand. Anal. data for **3** ($C_4H_5CuF_2N_2O$, MW = 198.64) Calcd: C, 24.19, H, 2.54, N, 14.10. Found: C, 24.31, H, 2.78, N, 14.59%. FTIR (KBr pellet/cm^{-1}): 3110br, 2949br, 1575s/sh, 1564s/sh, 1409s/sh, 1224sh, 1146sh, 1025sh, 881s, 822sh, 737s/sh, 689sh, 665s/sh cm^{-1}. Anal. data for **4** ($C_{16}H_{26}Cu_2F_2N_{10}O_{13}$, MW = 731.55) Calcd: C, 26.27, H, 3.58, N, 19.15. Found: C, 26.35, H, 3.70, N, 19.65%. FTIR (KBr pellet/cm^{-1}): 3098br, 1647w, 1579s/sh, 1558s/sh, 1402s/sh, 1354s, 1306s, 1219sh, 1043sh, 1019sh, 832s, 757s/sh, 689sh, 668sh cm^{-1}.

Magnetic Measurements. Variable-temperature (1.9−300 K) magnetic susceptibility and magnetization measurements on polycrystalline samples of **1**−**3** were carried out with a Quantum Design SQUID susceptometer using an applied magnetic field ranging from 0 to 5 T. Diamagnetic contribution of the constituent atoms of **1**−**3** per two copper(II) ions were estimated from Pascal's constants[21] as -380×10^{-6} (**1**), -263×10^{-6} (**2**), and -194×10^{-6} cm^3 mol^{-1} (**3**). A value of 60×10^{-6} cm^3 mol^{-1} was used for the temperature-independent paramagnetism of the copper(II) ion. The magnetic data were also corrected for the sample holder.

Computational Details. Calculations for compound **3** were performed through the Gaussian03 package using the B3LYP functional,[22] the quadratic convergence approach and a guess function generated with the Jaguar 6.5 code.[23] The triple-ζ all electron Gaussian basis sets proposed by Schaefer et al. were employed for the metal atoms.[24] Similar basis of double-ζ quality was used for the rest of the atoms.[24] More details about the use of the broken-symmetry (BS) approach to evaluate the magnetic coupling constants can be found in the literature.[25]

Since **3** is a periodic system with regular alternating bis-bidentate bpm and di-μ-fluoro bridges, two models have been built from the experimental crystal structure to evaluate the corresponding coupling constants. To avoid some electronic effects on the values of the calculated magnetic couplings when the periodic system is cut, we have included the nearest-neighbors metal ions in our models, being then the tetranuclear motifs **I** and **II** shown in Figure 1. Each model has been used to evaluate only one magnetic coupling, that is, the magnetic

dx.doi.org/10.1021/ic202740b | Inorg. Chem. 2012, 51, 4323−4334

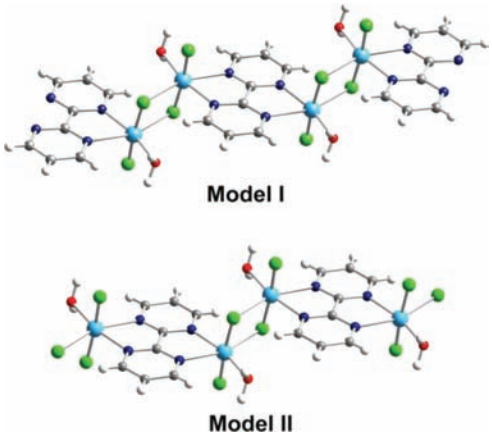

Figure 1. Models used in the evaluation of the magnetic exchange couplings through the bpm (J_a, top) and di-μ-fluoro (J_b, bottom) bridges in **3**. The copper, nitrogen, oxygen, fluoro, carbon, and hydrogen atoms are represented as pale blue, deep blue, red, green, gray, and white spheres, respectively.

interaction between the copper(II) ions placed in the middle of the molecular model of choice. With this in mind, DFT calculations have been done on the quintet state (++++) and the BS singlet states when the local spin moments on the right of the models are opposed to those on the left (++−−).

X-ray Crystallographic Analysis. X-ray diffraction data were collected with a Bruker-Nonius APEXII CCD area detector diffractometer using graphite-monochromated Mo-Kα radiation (α = 0.71073 Å). Data for compounds **1**−**4** were processed through the SAINT[26] reduction and SADABS[27] multiscan absorption softwares. The structures were solved by Patterson methods and subsequently completed by Fourier recycling using the SHELXTL software package.[28]All non-hydrogen atoms were refined anisotropically. The hydrogen atoms of the bpm ligand were placed in calculated positions and refined as riding atoms, while those on the water molecules (**1**−**4**) and hydroxo groups (**1**−**2**) were found and refined with restraints with a common fixed isotropic thermal parameter. The sulfate anion in **1** and, partially, the hexafluorosilicate anion in **2** were found disordered and modeled over multiple sites. Two sets of oxygen atoms (with occupancy factor of 0.5 each) were defined for the sulfate ion in **1**. These were first located on the ΔF map and then refined with restraints on bond lengths and angles. Similarly, two of the three independent fluoro atoms on the hexafluorosilicate anion in **2** [(F(2) and F(3)] were modeled over two positions, with refined occupancy factors of 0.262 and 0.773, respectively. The final full-matrix least-squares refinements on F^2, minimizing the function $\sum w(|F_o| - |F_c|)^2$, reached convergence with the values of the discrepancy indices given in Table 1. The final geometrical calculations were carried out with the PARST97[29] program whereas the graphical manipulations were performed with the DIAMOND[30] program and the XP utility of the SHELXTL system. CCDC reference numbers 843437−843440 (**1**−**4**). See Supporting Information for the crystallographic data in CIF format.

RESULTS AND DISCUSSION

Synthesis and IR characterization. The rational synthesis of alternating "ferro-antiferromagnetic" couplings in homometallic chains has been one of our reseach topics because of the difficulty of getting this uncommon spin topology in a regular alternating fashion. In general, the presence of a double hydroxo bridge in a dicopper(II) unit is one of the safest ways to get ferromagnetic coupling for values of the angle at the hydroxo bridge $\theta \leq 97.5°$. Two limitations concerning this unit are the need to work exclusively in aqueous media and to avoid the precipitation of copper(II) hydroxide. With counterions able to stabilize complexes with the same metal-to-bpm ratio found in the alternating chain of interest (i.e., 2:1), then, the

Table 1. Summary of the Crystal Data for $\{[Cu_2(\mu\text{-bpm})(H_2O)_4(\mu\text{-OH})_2][Mn(H_2O)_6](SO_4)_2\}_n$ (1), $\{[Cu_2(\mu\text{-bpm})(H_2O)_4(\mu\text{-OH})_2]SiF_6\}_n$ (2), $[Cu_2(\mu\text{-bpm})(H_2O)_2(\mu\text{-F})_2F_2]_n$ (3), and $[Cu(bpm)(H_2O)_2F(NO_3)][Cu(bpm)(H_2O)_3F]NO_3{\cdot}2H_2O$ (4)

	1	2	3	4
formula	$C_4H_{14}CuMn_{0.50}N_2O_{10}S$	$C_4H_8CuF_3N_2O_3Si_{0.5}$	$C_4H_5CuF_2N_2O$	$C_{16}H_{26}Cu_2F_2N_{10}O_{13}$
M_r	373.24	266.71	198.64	731.55
crystal system	monoclinic	monoclinic	monoclinic	monoclinic
space group	$P2_1/c$	$C2/c$	$P2_1/n$	Cc
a/Å	11.2224(3)	13.3364(8)	8.0661(1)	22.4518(4)
b/Å	8.2587(2)	8.2735(8)	7.6108(2)	14.2483(4)
c/Å	13.2628(4)	14.999(1)	10.0272(2)	8.6925(2)
α/deg	90	90	90	90
β/deg	99.2450(10)	97.258(5)	111.5350(10)	106.161(1)
γ/deg	90	90	90	90
V/Å^3	1213.26(6)	1641.8(2)	572.59(2)	2670.8(1)
Z	4	8	4	4
D_c/g cm^{-3}	2.043	2.158	2.304	1.819
T/K	298(2)	298(2)	295(2)	295(2)
F(000)	758	1064	392	1488
μ(Mo−Kα)/mm^{-1}	2.519	2.766	3.775	1.69
refl. collected	27905	23450	6212	14234
refl. indep. (R_{int})	4609 (0.0258)	3085 (0.0190)	1786 (0.0196)	7522 (0.0223)
refl. obs. [$I > 2\sigma(I)$]	3310	2641	1653	6904
$R_1{}^a$ [$I > 2\sigma(I)$] (all)	0.0347 (0.0506)	0.0238 (0.0280)	0.0198 (0.0221)	0.0251 (0.0283)
$wR_2{}^b$ [$I > 2\sigma(I)$] (all)	0.1039 (0.1149)	0.0759 (0.0809)	0.0561 (0.0570)	0.0600 (0.0612)
Flack parameter				0.003(6)
goodness-of-fit on F^2	1.046	1.065	1.139	0.996
$\Delta\rho_{max,\ min}$/e Å^{-3}	0.764/−0.765	0.735/−0.481	0.540/−0.252	0.274/−0.410

$^aR_1 = \sum||F_o| - |F_c||/\sum|F_o|$. $^bwR_2 = \{\sum w(F_o^2 - F_c^2)^2/\sum[w(F_o^2)^2]\}^{1/2}$ and $w = 1/[\sigma^2(F_o^2) + (mP)^2 + nP]$ with $P = (F_o^2 + 2F_c^2)/3$, m = 0.0567 (**1**), 0.0507 (**2**), 0.0249 (**3**), 0.0263 (**4**), and n = 0.8819 (**1**), 0.6186 (**2**), 0.2958 (**3**), 0.0000 (**4**).

dx.doi.org/10.1021/ic202740b | Inorg. Chem. 2012, 51, 4323−4334

fate of the reaction basically relies on the value of the pH of the solution. According to our experience,[11,31,32] the "ideal" pH for the formation of the alternating bpm/double hydroxo copper(II) chains resides in a small window, typically around 5.0, where precipitation of $Cu(OH)_2$ can already occur. The counterion of choice seems to have an influence on this pH, most likely because of crystal packing forces stabilizing a certain motif versus another. In the case of the nitrate counterion, three chain compounds of this type could be obtained in the past[11a,b] with the anion acting either as coordinating or noncoordinating group, proving that even small variations in the reaction conditions can be crucial for the final outcome.

In the course of synthetic attempts with the sulfate counterion, we noted the sporadic formation of small, blue hexagonal crystals (traces) together with big but very unstable dark green blocks (main product) identified as the dinuclear species $\{[Cu_2(bpm)_2(H_2O)_4(\mu\text{-}OH)_2]SO_4\cdot 11H_2O\}_n$. Preliminary structural investigations revealed the trace compound to be a chain with formula $\{[Cu_2(\mu\text{-}bpm)(H_2O)_4(\mu\text{-}OH)_2][Cu(H_2O)_6](SO_4)_2\}_n$.[31] In spite of the hygroscopicity/low stability of the dimer, fairly common for this class of complexes,[11,31−33] the chain, containing both sulfate and hexaaqua copper(II) ions, appeared particularly stable in air over time. Inspired by this finding, we sought to investigate the possibility to couple the sulfate anion with hexaaqua cations different from the elusive $[Cu(H_2O)_6]^{2+}$. This study provided us with the structure of complex **1**.

The reaction between $CuSO_4\cdot 5H_2O$, $MnSO_4\cdot H_2O$, and bpm in a 1:1:0.5 ratio resulted in the crystallization of green prismatic crystals of the previously reported 3D polymer $\{[Cu(bpm)(SO_4)]H_2O\}_n$[19c] together with a few royal blue hexagonal prisms of **1**, the starting pH of the mother liquor being around 4.8. Addition of NaOH to the initial reaction mixture to increase the pH value to 6.5−7.0 afforded crystals of complex **1** in a good yield [ca. 80% based on Cu(II)] with only a minimal precipitation of $Cu(OH)_2$ being observed in such conditions.

The parallel investigation of mixed bpm/halide systems going on in our laboratory during the course of this work inspired the synthesis of complex **2**. The in situ formation of hexafluorosilicate is known to occur through the slow decomposition of BF_4^- in water followed by the attack of the glass beaker by the fluoride ions.[34] The use by us of $Cu(BF_4)_2$ as the copper(II) source did not result here in the formation of alternating chains, though neither could we observe in situ formation of SiF_6^{2-} anions. Thus, we set out to explore the direct use of a fluoride salt as starting material, a procedure uncommon in the literature.[35] The reaction of stoichiometric amounts of $Cu(NO_3)_2\cdot 3H_2O$, bpm, and NaF [2:1:2 Cu(II)/bpm/F^- molar ratio] in water produced a blue microcrystalline precipitate after a few minutes of stirring of the reaction mixture under gentle heating (40 °C). Blue block crystals with matching infrared spectrum (IR) and microanalytical composition were then obtained by slow diffusion in a H-shaped tube of an aqueous solution of $Cu(NO_3)_2\cdot 3H_2O$ and bpm into an aqueous solution containing slight excess NaF over the course of two weeks, and identified as complex **2** by X-ray analysis.

Finally, complexes **3** (main product) and **4** (minor species) resulted from the reaction between $Cu(NO_3)_2\cdot 3H_2O$, bpm, and an organic fluoride salt (n-Bu_4NF) in ethanol at room temperature, the reaction being entirely conducted in a plastic vessel. Specifically, an excess of n-Bu_4NF [2:1:4 Cu(II):bpm:F^- molar ratio] was employed to increase the solubility of the bpm-bridged dicopper(II) unit in ethanol. Precipitation of possible "Cu-bpm" species was avoided by reacting copper(II) nitrate with the fluoride salt prior to the addition of the bpm ligand. Once formed, both complexes resulted totally insoluble in water, ethanol, or any other alcohol. Complex **3** was quite stable in the open air for weeks, while compound **4** undergoes a rapid crystal decomposition because of solvent loss. Of note, any effort to produce mixed bpm/Cl- or bpm/Br- 1D systems failed up to this point, the previously reported 2D honeycomb complexes $[Cu_2(\mu\text{-bpm})X_4]$[18a,b] being the only isolable products, regardless of the reaction conditions.

The bulk composition of **1**−**4** was determined via IR and elemental analysis, and confirmed by magnetic investigation (**1**−**3**). The most characteristic band in the IR spectra of complexes **1** and **2** is the strongly asymmetric doublet around 1580 cm^{-1}, diagnostic of a bridging bpm ligand, while a quasi-symmetric doublet typically associated with the presence of terminal chelating bpm appears at a similar frequency in the IR spectrum of complex **4**, as expected.[15a] A sharp, symmetric doublet centered at 1569 cm^{-1} is found in the spectrum of 3, which still features a bis-chelating bpm molecule: this apparent contradiction is due to the asymmetry of the bpm bridge in this complex, with each N_{bpm} atom occupying an equatorial or axial position in the metal coordination sphere. Intense bands indicative of the presence of uncoordinated sulfate or hexafluorosilicate anion in the spectra of **1** and **2** appear at 1068 cm^{-1} with shoulders at 1088 and 1042 cm^{-1}, and at 686 cm^{-1} with shoulders at 713 and 650 cm^{-1}, respectively.[36] Bands at 1354, 1306, and 832 cm^{-1} in the spectrum of **4** are due to the presence of the nitrate ion.[36]

Description of the Structures. $\{[Cu_2(\mu\text{-bpm})(H_2O)_4(\mu\text{-OH})_2][Mn(H_2O)_6](SO_4)_2\}_n$ (1) and $\{[Cu_2(\mu\text{-bpm})(H_2O)_4(\mu\text{-OH})_2]SiF_6\}_n$ (2). Compounds **1** and **2** consist of linear, cationic chains of copper(II) ions linked together by regular alternating coplanar bis-bidentate bpm and di-μ-hydroxo bridges (Figure 2).

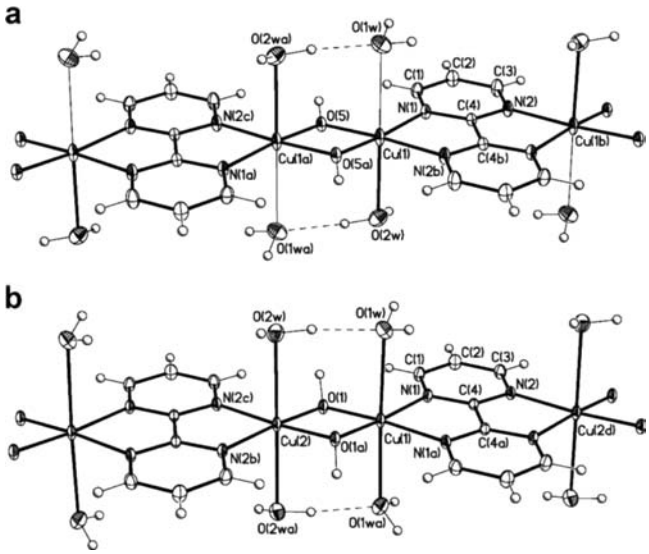

Figure 2. View of the alternating μ-bpm/di-μ-hydroxo copper(II) chains running along the b axis in both **1** (a) and **2** (b) with the atom numbering scheme. Thermal ellipsoids are plotted at the 30% probability level. [Symmetry codes for **1**: (a) = 1−x, 2−y, −z; (b) = 1−x, 1−y, −z; (c) = x, 1+y, z. Symmetry codes for **2**: (a) = 1−x, y, −0.5−z; (b) = 1−x, 1+y, −0.5−z; (c) = x, 1+y, z; (d) = x, 1−y, z].

Charge balance is provided by either sulfate (**1**) or hexafluorosilicate (**2**) anions. In the case of **1**, discrete $[Mn(H_2O)_6]^{2+}$

dx.doi.org/10.1021/ic202740b | Inorg. Chem. 2012, 51, 4323−4334

cations are also present. **1** crystallizes in the monoclinic space group $P2_1/c$, whereas **2** packs with symmetry $C2/c$, with minor implications on the copper atoms environments (vide infra). In both cases, the chains grow along the crystallographic *b* axis. The two linear motifs are akin to each other and very similar to the perchlorate-containing species of formula $\{[Cu_2(\mu\text{-bpm})(H_2O)_4(\mu\text{-OH})_2](ClO_4)\cdot 2H_2O\}_n$, whose magnetic properties were subject of the early report by Hatfield et al.,[11c] while their skeleton somewhat differs from the literature linear or *quasi*-linear nitrate-containing compounds $\{[Cu_2(\mu\text{-bpm})(\mu\text{-OH})_2(NO_3)_2]\cdot 2H_2O\}$ (**5a**),[11a,b] $\{[Cu_2(\mu\text{-bpm})(H_2O)_2(\mu\text{-OH})_2](NO_3)_2\}$ (**5b**),[11b] and $\{[Cu_2(\mu\text{-bpm})(H_2O)_2(OH)_2(NO_3)_2]\cdot 2H_2O\}$ (**5c**),[11b] basically because of the presence of a coordinating counterion (**5a** and **5c**) and/or five-coordinated metal ions (**5a** and **5b**) in these latter cases.

Each copper(II) ion in **1** and **2** adopts a distorted CuN_2O_4 octahedral coordination, where two N_{bpm} and two O_{OH} atoms form the equatorial plane, while two water molecules are coordinated in the axial positions, with final (4 + 1 + 1) or (4 + 2) geometries for **1** and **2**, respectively. The equatorial $Cu-O_{OH}$ [1.930(1)−1.939(1) Å in **1** and 1.919(1)−1.920(1) Å in **2**] and $Cu-N_{bpm}$ [2.025(2)−2.036(2) Å in **1** and 2.037(1) Å in **2**] bond distances are in agreement with the values found in **5a**, **5b**, and **5c**.[11a,b] The axial $Cu-O_w$ bonds are significantly longer, but they remain within the literature values [2.609(2) and 2.445(2) Å for Cu(1)−O(1w) and Cu(1)−O(2w) in **1**, 2.583(1); 2.557(1) Å for Cu(1)−O(1w) and Cu(2)−O(2w) in **2**]. The largest deviations from the N(1)N(2b)O(5)O(5a) (**1**) and N(1)N(1a)O(1)O(1a) and N(2b)N(2c)O(1)O(1a) (**2**) equatorial mean planes are 0.099(1), 0.103(1), and 0.095(1) Å, respectively.

The copper atoms lie in the basal plane in **2**, while they are displaced by 0.029(1) Å toward the O(2w) water molecule in **1**. The dihedral angle between the dihydroxo-dicopper unit [Cu(1)Cu(1a)O(5)O(5a) in **1**, Cu(1)Cu(2)O(1)O(1a) in **2**] and the metal equatorial plane is about 4.5° in **1** and 4.2° in **2** [values for **5a**, **5b**, and **5c** are 3.0, 5.9, and 4.1°, respectively].[11a,b]

The bridging bpm ligand, as a whole, is planar in both complexes, and its bond distances and angles are as expected. The angles subtended at the copper atom by the chelating bpm are 82.0(1)° (**1**) and 81.7(1)−81.8(1)° (**2**), values which are very close to those found in complexes **5a**−**5c** [range 81.4−81.9°].[11a,b] Two adjacent bpm ligands are perfectly coplanar, for symmetry reasons.

The metal−metal separations through the di-μ-hydroxo bridge in **1** and **2** [2.832(1) and 2.824(1) Å, respectively] are shorter than those found in **5a** [2.886(1) Å], **5b** [2.854(1) Å], and **5c** [2.860(1) Å]. Consequently, the angles at the hydroxo bridge [θ = 94.1(1)° in **1** and 94.7(1)° in **2**], are smaller than those in **5a**, **5b**, and **5c** [96.2(2), 96.1(2), and 95.0(1)°, respectively].[11a,b] The intrachain copper−copper separations through bpm are 5.428(1) (**1**) and 5.449(1) Å (**2**). Again, these values are somewhat shorter than the corresponding ones in **5a** [5.471(1) and 5.474(1) Å], **5b** [5.461(2) Å], and **5c** [5.452(2) Å].[11a,b]

In both compounds, a combination of intra- and interchain hydrogen bonds involving the coordinated water molecules results in the formation of a linear "*C2*" motif.[37a] By linking adjacent copper(II) chains together, these interactions give rise to supramolecular 2D layers that extend parallel to the *bc* (**1**) *ab* (**2**) planes (Figure 3). The sulfate (**1**) and hexafluorosilicate (**2**) groups further stabilize these motifs, generating a water-counterion H-bonding pattern in which supramolecular six-membered rings [$O_4O'_2$ (**1**) and O_4F_2 (**2**)] can be noted, which

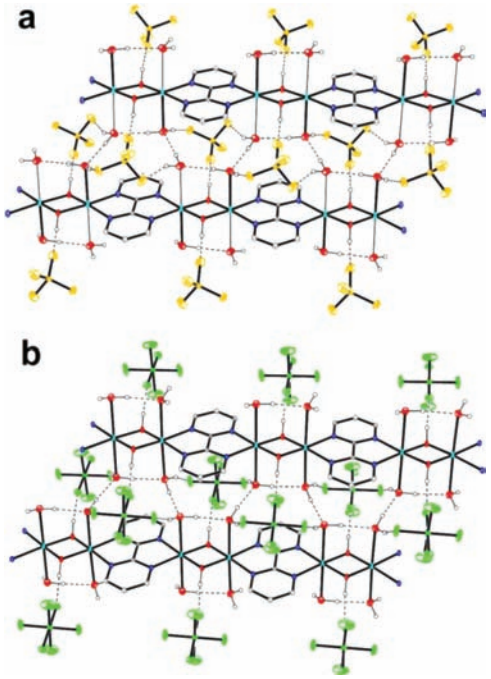

Figure 3. View of the supramolecular 2D motifs growing in the *bc* (**1**, **a**) and *ab* (**2**, **b**) planes. Hydrogen bonds are shown as dashed lines. Sulfate (**1**) and hexafluorosilicate (**2**) ions are depicted in yellow and green, respectively; for clarity, only one set of atoms is shown for each ion. The hydrogen atoms of the bpm molecules are omitted.

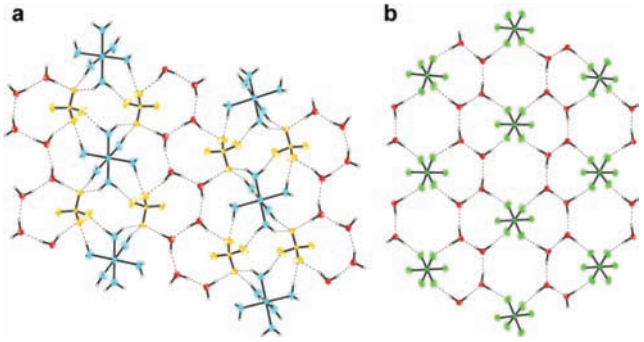

Figure 4. Supramolecular 2D motifs generated through hydrogen bonds (dashed lines) between water molecules and counterions in **1** (**a**) and **2** (**b**). Sulfate (**1**) and hexafluorosilicate (**2**) ions are depicted in yellow and green, respectively; for clarity, only one set of atoms is shown for each ion. Hexaaqua manganese(II) cations in **1** are depicted in sky blue.

grow into "*T6(2)*" *tapes*[37b] by sharing two water molecules with each adjacent ring (Figures 3 and 4). Neighboring water-counterion T6(2) tapes in the *ab* (**1**) and *bc* (**2**) planes are either joined together by means of hydrogen bonds with the hexaaqua manganese(II) cations (**1**) or connected through the hexafluorosilicate anions (**2**), each one participating with a total of four F atoms (2 + 2) to the closure of two vicinal rings.

This creates more or less complicated water-counterion extended layers, as shown in Figure 4, which lie between the (di-μ-hydroxo)(μ-bpm)copper(II) chains and are connected to them through the coordinated water molecules, ensuring the supramolecular 3D arrangement. Additional hydrogen bonds between the hydroxo and the sulfate (**1**) or hexafluorosilicate (**2**) groups, further contribute to the cohesion between the

dx.doi.org/10.1021/ic202740b | *Inorg. Chem.* 2012, 51, 4323−4334

supramolecular layers containing the copper(II) chains and those containing the counterions and the coordinated water molecules.

$[Cu_2(\mu\text{-bpm})(H_2O)_2(\mu\text{-F})_2F_2]_n$ (3). The structure of **3** consists of "step like" chains of copper(II) ions with regular alternating perpendicular bis-bidentate bpm and di-μ-fluoro bridges. Each copper atom in **3** has a distorted CuN_2O_4 octahedral (4 + 1 + 1) coordination: one N_{bpm} [N(1)], a water molecule [O(1w)], one bridging [F(1b)], and one terminal [F(2)] fluorine atom form the equatorial plane, with the second bpm-nitrogen [N(2a)] and bridging fluoro [F(1)] atoms occupying the axial positions (Figure 5). As a consequence, adjacent

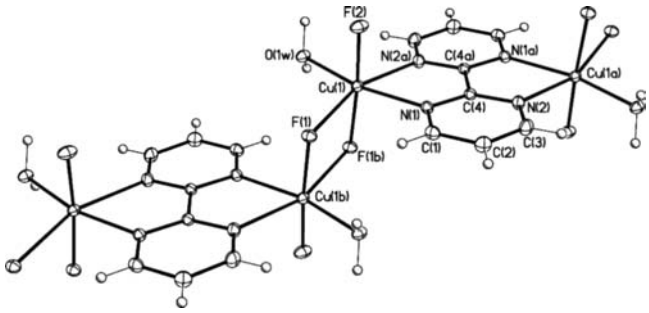

Figure 5. View of the alternating chain **3** with the atom numbering scheme. Thermal ellipsoids are plotted at the 30% probability level. [Symmetry codes: (a) = 1−*x*, 2−*y*, −*z*; (b) = 2−*x*, 2−*y*, −*z*].

copper equatorial planes are parallel to each other and basically perpendicular to both the bpm and di-μ-fluoro bridges [dihedral angles of 89.2(1) and 94.1(1)°, respectively].

The di-μ-fluoro bridge is asymmetric, with each fluoro atom simultaneously occupying either an equatorial or one axial site at the metal atoms in the di-μ-fluorodicopper unit, with Cu−F distances coherent with literature values [$Cu-F_{eq}$ = 1.917(1) and $Cu-F_{ax}$ = 2.336(1) Å]. The $Cu-N_{bpm}$ and $Cu-O_w$ also assume expected values. The bpm bridging ligand, as a whole, is planar, and its bond distances and angles are as expected. The angle subtended at the copper atom by the bridging bpm ligand is 74.1(1)°, a value which as far as we know, is the shortest one observed in Cu-bpm complexes. Two adjacent bpm ligands are parallel, with a plane-to-plane distance of about 1.94 Å.

The intrachain metal−metal separations are 5.925(1) (through bpm) and 3.303(1) Å (across the di-μ-F bridge). The shortest Cu−Cu distances observed for **1** and **2** (5.428 and 5.449 Å) are significantly shorter than the corresponding observed for **3**. This is because the nitrogen atoms of the bpm in compounds **1**−**2** are in the equatorial position whereas the copper atom in **3** has a distorted CuN_2O_4 octahedral coordination, in which only one N_{bpm} nitrogen atom occupies the equatorial plane, with the second bpm-nitrogen atom occupying the axial position.

Each chain, in **3**, interacts with a total of four neighboring ones by means of extensive hydrogen bonds in which the coordinated water molecules act as donor toward both bridged and terminal fluoro atoms (Figure 6a). Adjacent chains are virtually rotated with respect to each other by 180° around the crystallographic *b* axis (see Figure 6b), this orientation precluding the formation of a 2D building similar to that found in the $[Cu_2(\mu\text{-bpm})X_4]$ compounds [X = Cl^- and Br^-].[18a,b]

$[Cu(bpm)(H_2O)_2F(NO_3)][Cu(bpm)(H_2O)_3F]NO_3\cdot 2H_2O$ (4). Compound **4** is a discrete species comprised by two distinct mononuclear units, one neutral and the other positively

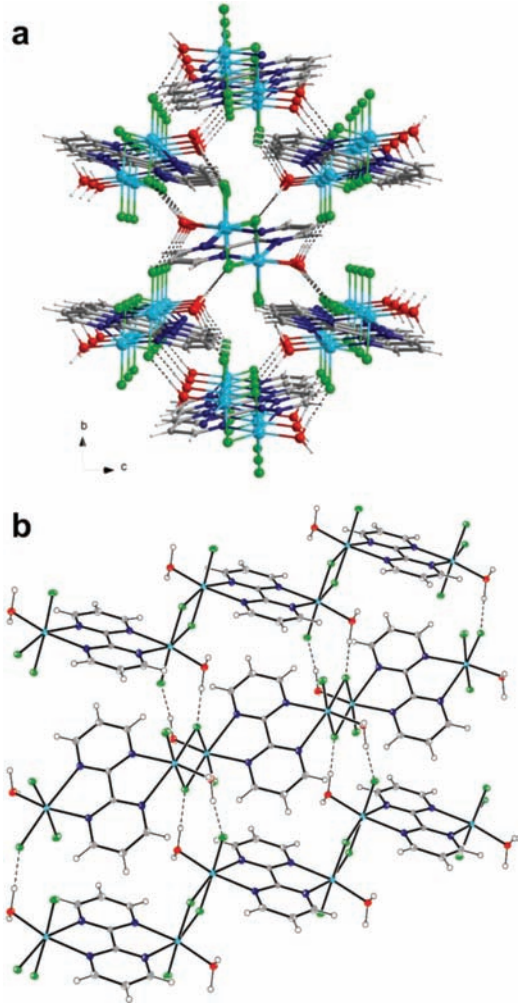

Figure 6. (a) View of the crystal packing of **3** along the crystallographic *a* axis. (b) A view of the respective orientation of adjacent chains in **3**. The hydrogen bonds are drawn as dashed lines.

charged with formula $[Cu(bpm)(H_2O)_2F(NO_3)]$ and $[Cu(bpm)(H_2O)_3F]^+$, respectively (see Figure 7). Charge balance

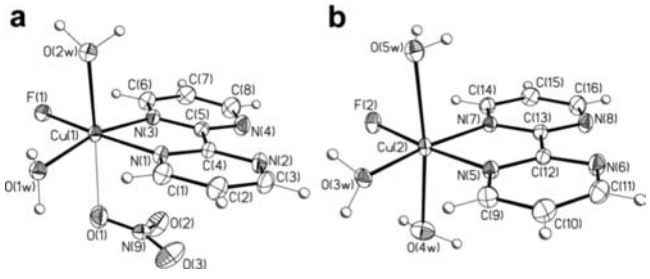

Figure 7. Crystal structure of the neutral (a) and cationic (b) mononuclear units in complex **4** with the atom numbering scheme. Thermal ellipsoids are plotted at the 30% probability level.

is reached by means of a free nitrate anion. A total of two extra water molecules of crystallization per asymmetric unit are also present in the structure.

In each mononuclear unit, the copper(II) ions [Cu(1) and Cu(2)] are six-coordinated with two N_{bpm} atoms, three oxygen atoms, and a fluoro atom building an elongated octahedral environment. The major difference between the two units

dx.doi.org/10.1021/ic202740b | *Inorg. Chem.* 2012, 51, 4323−4334

resides in one of the axial positions, occupied by a nitrate anion in one case and a water molecule in the other.

The equatorial planes around Cu(1) [N(1)N(3)F(1)O(1w)] and Cu(2) [N(5)N(7)F(2)O(3w)] are differently distorted with main deviations from planarity of about 0.12 and 0.04 Å, respectively. The Cu(1) ion is displaced by 0.123 Å out of its equatorial plane, toward the axial O(2w) molecule, a deviation which does not occur in the cationic unit.

The equatorial Cu−O_w bond lengths [1.973(1)−1.959(2) Å] are close to those reported for other copper(II) complexes containing terminal water molecules in the equatorial position. The axial Cu−O_w bond distances [range 2.300(2)−2.459(2) Å] are significantly shorter than the Cu−$O_{nitrate}$ [2.640(2) Å], but these values are all very close to those reported for similar copper(II) complexes. The equatorial Cu−N_{bpm} bond lengths [range 1.995(2)−2.022(2) Å] are as expected, as well.

The bpm molecules as a whole are planar [max. deviations from mean planes are around 0.03−0.04 Å], and they form dihedral angles of 10.28(3) and 3.53(4)° with the copper equatorial planes in the neutral and cationic units, respectively.

The large number of water molecules in the structure (coordinated and free) induces the formation of an extended network of hydrogen bonds in the overall crystal packing. In particular, hydrogen bonds involving bound and free nitrate anions, coordinated [O(1w), O(2w), O(4w), O(5w)] and crystallization [O(6w)] water molecules lead to the formation of a supramolecular *pseudo*-helical 1D motif running down the crystallographic *a* axis. $NO_3^-\cdots\pi$ type interactions also contribute to stabilize this motif, with the coordinated nitrate groups sandwiched between the bpm molecules of consecutive units and, conversely, some of the bpm molecules placed between a coordinated and a noncoordinated nitrate group (Figure 8).

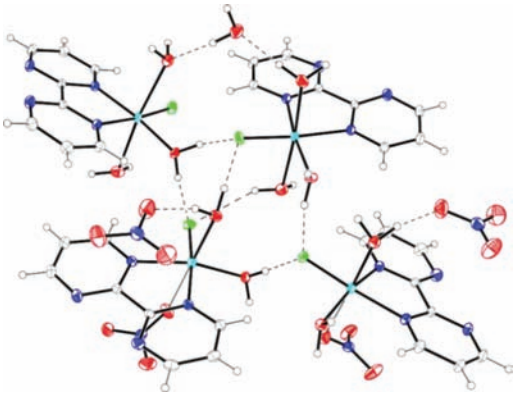

Figure 8. Fragment of the crystal packing of **4** showing, in particular, the hydrogen bonding interactions (dashed lines) between adjacent units in the *ab* plane.

Further hydrogen bonds also involving fluoro and N_{bpm} atoms link adjacent chains in the *ab* plane, the shortest copper−copper separation being 5.449(2) Å [Cu(1)···Cu(2a): (a) = *x*, −1−*y*, −0.5+*z*]. Finally, hydrogen bonding interactions between the free O(7w) and coordinated O(5w) water molecules ensure the cohesion of the crystal lattice in the third dimension.

Magnetic Properties of 1−3. The description and discussion of the magnetic properties of **1** and **2** will be performed first because of their structural similarity [chains of copper(II) ions with regular alternating bpm and di-μ-hydroxo bridges] and then, the magnetic behavior of **3** (where the alternating bridges are bpm and two fluoride anions) will be detailed. In this latter case, DFT type calculations on metal fragments are also included to substantiate and properly assign the magnetic couplings obtained by fit.

Compounds 1 and 2. The magnetic properties of **1** under the form of $\chi_M T$ versus *T* plot [χ_M is the magnetic susceptibility per two copper(II) ions] are shown in Figure 9. At room temperature $\chi_M T$ for **1** is 5.18 $cm^3\ mol^{-1}\ K$, a value which is somewhat below that expected for two noninteracting copper(II) ions plus a magnetically isolated spin sextet from a manganese(II) ion [$\chi_M T = g_{Cu}^2 S_{Cu}(S_{Cu}+1)/4 + g_{Mn}^2 S_{Mn}(S_{Mn}+1)/8$ = 5.28 $cm^3\ mol^{-1}\ K$ with S_{Cu} = 1/2, S_{Mn} = 5/2, g_{Cu} = 2.08, and g_{Mn} = 2.0]. This value continuously decreases upon cooling to reach a quasi plateau below 30 K with a value of $\chi_M T$ which is close to that expected for a spin sextet magnetically isolated, and it decreases slightly in the very low temperatures domain. This curve corresponds to an overall antiferromagnetic coupling between the copper(II) ions, the presence of the hexaaqua manganese(II) cation in the structure accounting for the plateau at low temperatures. The small decrease at the lower limit of the temperatures would be due to very weak antiferromagnetic interactions between the spin sextets of the fully solvated manganese(II) cations.

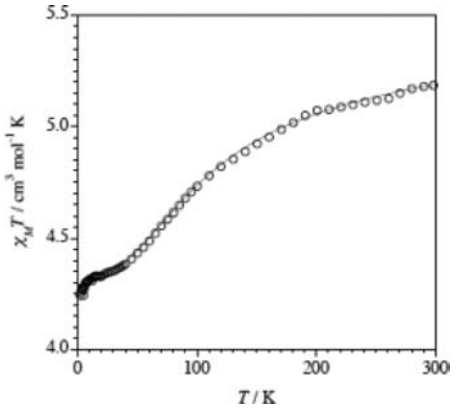

Figure 9. Thermal variation of the $\chi_M T$ product for complex **1**: (○) experimental data; (solid line) best-fit curve (see text).

Given the well-known ability of the bpm molecule to mediate relatively important antiferromagnetic interactions between copper(II) ions (antiferromagnetic couplings ranging from −236 to −132.2 cm^{-1} were reported between copper(II) ions linked across bis-bidentate bpm when the σ in-plane $d_{x^2-y^2}$ exchange pathway is operative),[11,13b,15c,16a,18a,b,20b,33,38−42] it is clear that the local spin doublets of the -Cu^{II}(μ-bpm)Cu^{II}- intrachain fragment will tend to cancel each other. As far as the di-μ-hydroxodicopper(II) fragment is concerned, the relatively large ferromagnetic interactions observed through this double bridge in the dinuclear complexes of formula $[Cu_2(bpm)_2(H_2O)_2(\mu\text{-}OH)_2(NO_3)_2]\cdot 4H_2O$ (J = +114 cm^{-1})[11a,b] and $[Cu_2(bpm)_2(H_2O)_4(\mu\text{-}OH)_2](ClO_4)_2\cdot 4H_2O$ (J = +147 cm^{-1})[33] (see Table 2) with the Hamiltonian being defined as $\boldsymbol{H} = -J\,\boldsymbol{S}_A\cdot\boldsymbol{S}_B$, which nicely fit the well-known Hatfield and Hogdson's correlation between J and the angle at the hydroxo bridge (θ) that predicts a ferromagnetic coupling for $\theta \leq 97.5°$,[20] strongly support a significant ferromagnetic interaction within this motif in **1**. Consequently, the magnetic susceptibility data of **1** were analyzed with the Hamiltonian $\boldsymbol{H} = -J\sum_{i=1}^{n/2}(\boldsymbol{S}_{2i}\cdot\boldsymbol{S}_{2i-1} - \alpha\boldsymbol{S}_{2i}\cdot\boldsymbol{S}_{2i+1})$ were J is the exchange coupling parameter associated with a

dx.doi.org/10.1021/ic202740b | *Inorg. Chem.* 2012, 51, 4323−4334

Table 2. Selected Magneto-Structural Data for Dinuclear or 1D Di-μ-hydroxo-bridged Copper(II) Complexes Containing Terminal or Bridging bpm, Respectively[a]

compound	Cu−O/Å	Cu−N/Å	Cu···Cu[b]/Å	θ[c]/deg	τ[d]/deg	J_F[e]/cm^{-1}	J_{AF}[f]/cm^{-1}	ref
$[Cu_2(bpm)_2(H_2O)_2(\mu\text{-}OH)_2(NO_3)_2]\cdot 4H_2O$	1.944	2.016	2.881/-	95.7	61.3	+114		11a, b
$[Cu_2(bpm)_2(H_2O)_4(\mu\text{-}OH)_2](ClO_4)_2\cdot 2H_2O$	1.947	2.021	2.870/-	95.0	57.8	+147		33
$\{[Cu_2(\mu\text{-}bpm)(\mu\text{-}OH)_2(NO_3)_2]\cdot 2H_2O\}_n$ (**5a**)	1.926	2.045	2.886/5.473	96.2	37.1	+105	−140	11a, b
$\{[Cu_2(\mu\text{-}bpm)(H_2O)_2(\mu\text{-}OH)_2](NO_3)_2\}_n$ (**5b**)	1.922	2.043	2.854/5.461	95.9	59.6	+97.5	−135	11b
$\{[Cu_2(\mu\text{-}bpm)(H_2O)_2(\mu\text{-}OH)_2(NO_3)_2]\cdot 2H_2O\}_n$ (**5c**)	1.940	2.039	2.860/5.452	95.0	60.2	+160	−145	11b
$\{[Cu_2(\mu\text{-}bpm)(H_2O)_4(\mu\text{-}OH)_2][Mn(H_2O)_6](SO_4)_2\}_n$ (**1**)	1.934	2.030	2.832/5.428	94.2	57.9	+194	−149	this work
$\{[Cu_2(\mu\text{-}bpm)(H_2O)_4(\mu\text{-}OH)_2]SiF_6\}_n$ (**2**)	1.920	2.037	2.824/5.449	94.8	53.0	+176	−141	this work

[a]Average bond distances and angles are given for each structure. [b]Copper−copper separation across di-μ-hydroxo/μ-bpm bridges. [c]θ = angle at the hydroxo bridge. [d]τ = out-of-plane displacement of the hydroxo-hydrogen from the Cu_2O_2 plane. [e]Magnetic coupling through the di-μ-hydroxo bridge. [f]Magnetic coupling across the μ-bpm bridge.

particular copper(II) pair and αJ is the exchange constant assigned to the adjacent unit (the alternating parameter α being defined as the $J_F/|J_{AF}|$ quotient). The treatment of the magnetic data of **1** was done by a previously reported numerical expression derived by Georges et al.[43] and based on closed spin chains of increasing length (the calculations were limited up to 14-spin rings with local spin doublets). The corresponding Curie law term for a $S = 5/2$ (that is, $N\beta^2 g_{Mn}{}^2[S_{Mn}(S_{Mn}+1)]/3kT$) was added to the numerical expression to account for the presence of the $[Mn(H_2O)_6]^{2+}$ cation. The best-fit parameters through the analysis of the magnetic data of **1** in the temperature range 300−10 K are: $J_{AF} = -149$ cm^{-1}, $J_F = +194$ cm^{-1}, $g_{Cu} = 2.08$, and $g_{Mn} = 1.99$. The computed curve matches very well the magnetic susceptibility data of **1**, as shown by the solid line in Figure 9.

The magnetic properties of **2** under the form of χ_M versus T plot [χ_M is the magnetic susceptibility per two copper(II) ions] are shown in Figure 10. $\chi_M T$ for **2** at 300 K is 0.74 cm^3 mol^{-1} K,

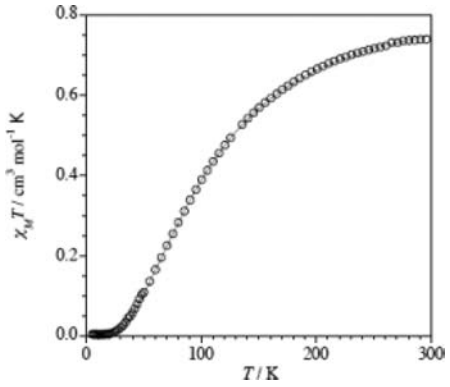

Figure 10. Thermal variation of of χ_M (○) for complex **2**. The solid line is the best-fit curve; (○) experimental data; (solid line) best-fit curve (see text).

a value which is slightly below that calculated for two magnetically noninteracting copper(II) ions. This value continuously decreases upon cooling, and it practically vanishes at 20 K. A rounded maximum of the magnetic susceptibility which is centered at about 114 K occurs. The coexistence of relatively important intrachain antiferro- (through bridging bpm) and ferromagnetic (across the di-μ-hydroxo bridge) is expected for **2** in the light of the analysis done for **1**. Consequently, the analysis of the magnetic data of **2** were analyzed through the above-mentioned numerical expression leading to the following best-fit parameters: $J_{AF} = -141$ cm^{-1}, $J_F = +176$ cm^{-1} and $g_{Cu} = 2.08$. The computed curve (solid line in Figure 10) reproduces well the magnetic data in the whole temperature range investigated. Relevant magneto-structural data dealing with copper(II) complexes containing bidentate or bis-bidentate bpm and di-μ-hydroxo bridges are listed in Table 2. One can see in this Table that relatively large ferro- and antiferromagnetic interactions between the copper(II) ions are mediated by the di-μ-hydroxo and bis-bidentate bpm, respectively. Both the nature and magnitude of the magnetic coupling in these systems have been rationalized on an orbital basis.[44] So, the ferromagnetic coupling observed in the di-μ-hydroxodicopper(II) complexes for $\theta \leq 97.5°$ is due to the accidental orthogonality of the magnetic orbitals ϕ_A and ϕ_B which describe the unpaired electron on each copper(II) ion (ϕ_A and ϕ_B being $d_{x^2-y^2}$ type magnetic orbitals delocalized on the equatorial bpm-nitrogen and hydroxo-oxygen atoms). The overall overlap integral $S = \langle\phi_A|\phi_B\rangle$ is close to zero for values of θ where the orthogonality occurs, and the singlet−triplet energy gap, which is approximated by the expression $J = 2j + 4\beta S$ [j is the bielectronic integral $\langle\phi_A(1)\ \phi_B(2)|e^2/r_{12}|\phi_A(2)\ \phi_B(1)\rangle$], is governed by the positive $2j$ term. The relatively large antiferromagnetic coupling between copper(II) ions separated by about 5.4 Å through bis-bidentate bpm (J_{AF} in Table 2) is due to the strong σ in-plane overlap between the above-mentioned $d_{x^2-y^2}$ type magnetic orbitals centered on each copper(II) ion.[11,13b,15c,16a,18a,b,20b,33,38−42] The values of J_{AF} in Table 2 vary in a very narrow range as expected in the light of the similarity of the structural parameters of the Cu(μ-bpm)Cu unit. This is not the case for those of J_F which are strongly dependent on small variations of θ, their values increasing as far as θ decreases. The values of J_F for complexes **1** and **2** are the largest ones in the series, and they constitute suitable examples to support the conclusion of Ruiz et al.[25a] about the existence of a correlation between the out-of-plane displacement of the hydrogen atom of the hydroxo bridge (τ) and θ: a large τ value [55 (**1**) and 53° (**2**)] is associated with a small θ [94.2 (**1**) and 94.8 (**2**)°], which also favors a more positive value of the magnetic coupling [+194 (**1**) and +176 cm^{-1} (**2**)].

Compound 3. The magnetic properties of **3** under the form of $\chi_M T$ and χ_M versus T plots [χ_M is the magnetic susceptibility per two copper(II) ions] are shown in Figure 11. At 300 K $\chi_M T$ is 0.84 cm^3 mol^{-1} K, a value which is expected for two magnetically noninteracting spin doublets. Upon cooling, this value decreases first smoothly until 80 K and then abruptly at lower temperatures to reach a value of 0.20 cm^3 mol^{-1} K at 1.9 K. The magnetic susceptibility exhibits a sharp maximum at 8.0 K (see inset of Figure 11). These features are as expected for an overall weak antiferromagnetic interaction between the copper(II) ions.

dx.doi.org/10.1021/ic202740b | Inorg. Chem. 2012, 51, 4323−4334

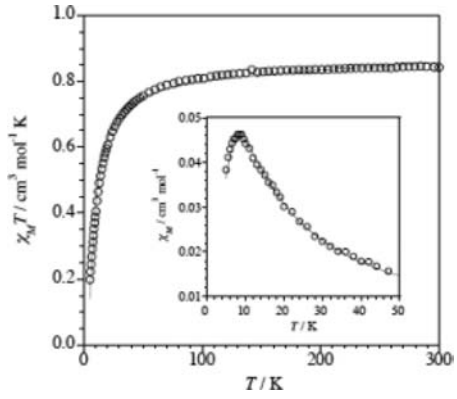

Figure 11. Thermal variation of the $\chi_M T$ (○) product for complex **3**. The inset shows the χ_M (○) versus T plot in the low temperature domain. The solid line is the best-fit curve through eq 1 (see text).

According to the structure of **3**, regular alternating bis-bidentate bpm and di-μ-fluoro bridges, its magnetic behavior would obey that of an alternating chain. All our attempts to fit the magnetic data of **3** through the numerical expression used above or an alternating AF-F chain failed and only a good match of the susceptibility data was achieved by means of the alternating AF-AF chain model, the Hamiltonian being defined as $\boldsymbol{H} = -J\sum_{i=1}^{n/2}(\boldsymbol{S}_{2i}\cdot\boldsymbol{S}_{2i-1} + \alpha\boldsymbol{S}_{2i}\cdot\boldsymbol{S}_{2i+1})$. In this Hamiltonian, J and αJ are the two magnetic couplings and α is the alternation parameter. The corresponding analytical expression for the analysis of the susceptibility data of **3** which was derived by Hatfield et al. is given by eq 1[45]

$$\chi_M = (N\beta^2 g^2/kT)[(A + Bx + Cx^2)/(1 + Dx + Ex^2 + Fx^3)] \quad (1)$$

with $x = |J|/kT$ and the $A-F$ coefficients for $0 \le \alpha \le 0.4$ being expressed by eqs 2−7

$$A = 0.25 \quad (2)$$

$$B = -0.062935 + 0.11376\alpha \quad (3)$$

$$C = 0.0047778 - 0.033268\alpha + 0.12742\alpha^2 - 0.32918\alpha^3 + 0.25203\alpha^4 \quad (4)$$

$$D = 0.053860 + 0.70960\alpha \quad (5)$$

$$E = -0.00071302 - 0.10587\alpha + 0.54883\alpha^2 - 0.20603\alpha^3 \quad (6)$$

$$F = 0.047193 - 0.0083778\alpha + 0.87256\alpha^2 - 2.7098\alpha^3 + 1.9798\alpha^4 \quad (7)$$

Least-squares best-fit parameters through eq 1 for **3** are $J = -8.1$ cm^{-1}, $\alpha J = -0.30$ cm^{-1}, and $g = 2.09$. The calculated curve reproduces very well the magnetic data in the whole temperature range investigated (see solid line in Figure 11).

Two important questions concerning these weak magnetic couplings obtained by fit are in order: (i) the first one deals with the justification of their weakness and (ii) the second one is their unambiguous assignment to each bridge. A simple orbital picture provides a clear-cut answer to the first point. As shown in Figure 12, the unpaired electron on each copper(II) ion in **3** is of the $d_{x^2-z^2}$ type [the x and z axes being roughly defined by the equatorial Cu(1)−N(1) and Cu(1)−F(2) bonds] and consequently, the spin density on the axial sites

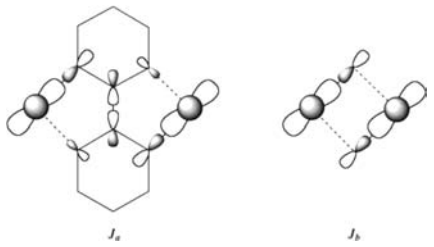

Figure 12. Scheme showing the arrangement of the interacting magnetic orbitals through the bis-bidentate bpm (left) and di-μ-fluoro bridges (right) in **3**.

[F(1) and N(2A)] is predicted to be very small. The two magnetic orbitals are then localized in parallel planes which are perpendicular to the mean bpm plane (in contrast to what occurred in **1** and **2** where they were all coplanar) and to the Cu(μ-F)$_2$Cu skeleton, and because of the inversion center in the two bridging pathways, a very poor overlap is predicted. Consequently, according to the Kahn's model where the antiferromagnetic coupling is proportional to the square of the overlap integral between the magnetic orbitals for a dicopper(II) unit,[44] a weak magnetic coupling would be expected through these out-of-plane exchange pathways.

Theoretical DFT calculations have been performed on the dinuclear models **I** and **II** of **3** (see Figure 1) to provide additional support to the small size of the observed magnetic couplings as well as to assign them to the respective bridges. The values computed for J_a and J_b are +0.3 and −4.4 cm^{-1}, respectively. They compare well with the values obtained by fit although somewhat shifted toward less negative values (see Table 3). In the light of these results, it seems clear that the larger coupling is mediated by the di-μ-fluoro bridge and that it is antiferromagnetic. Values of the magnetic coupling not larger than 0.4 cm^{-1} were reported for a small number of magneto-structurally characterized di-μ-fluorodicopper(II) complexes exhibiting the same out-of plane exchange pathway.[46] The somewhat larger magnetic coupling in **3** through the difluoro bridges is most likely due to the larger value of the angle at the fluoro bridge [101.4(1)° in **3** versus values varying in the range 93.73(8)−97.19(8)° in the previous examples]. Finally, as far as the very weak ferromagnetic interaction calculated for the other pathway, its value is so small that most likely, its sign is physically meaningless.

Table 3. Selected Structural Parameters [Å and deg] for the Bridging Ligands (L_i) and Theoretical and Experimental Magnetic Coupling Constants (cm^{-1}) in 3[a]

J_i	L_i	Cu−X_1	Cu−X_2	Cu···Cu	Cu−F−Cu	J_{B3LYP}	J_{exp}
J_a	μ-bpm	2.070	2.401	5.925		+0.3	−0.3
J_b	di-μ-F	1.917	2.336	3.303	101.4	−4.4	−8.1

[a] X_1 and X_2 represent the two L_i atoms involved in the bridge [i.e., N(1), N(2) for bpm and F(1), F(1b) for the di-μ-fluoro moiety, respectively].

CONCLUSIONS

In this work, three novel 1D copper(II) compounds are presented. Two of these (**1** and **2**) show alternation of ferro- and antiferromagnetic couplings through the di-μ-hydroxo and μ-bpm bridges, and constitute rare examples of compounds of this kind. In fact, structural data are available only for other

dx.doi.org/10.1021/ic202740b | Inorg. Chem. 2012, 51, 4323−4334

three parent compounds, all of which contain nitrate counterions. The paucity of such type of complexes in the literature should be attributed mainly to synthetic difficulties. The polymerization of the μ-bpm-dicopper(II) unit via di-μ-hydroxo bridges is particularly sensitive to the reaction pH, and often in competition with either the undesired precipitation of insoluble $Cu(OH)_2$ or the formation of alternative Cu(II)-bpm species. The choice of the counterion has been proved to be crucial not just for the stabilization of the crystal packing but also for the magnetic properties exhibited by such arrangements. At the very bottom, given the dependence of the magnetic coupling in the di-μ-hydroxo-dicopper(II) fragment on the Cu−OH−Cu (θ) angle, it should be noted that "not-ideal" counterions directing the system toward a more classical situation, with two alternating J_i and J_{i+1} coupling constant of the same sign (antiferro), could eventually be found. Apart from the published examples containing nitrate, alternating di-μ-hydroxo/μ-bpm bridged copper(II) chains have been occasionally observed in our laboratory also in the presence of counterions like perchlorate, sulfate, or triflate, as well as sulfate/hexaaqua copper(II) ions, but magnetic studies could not been performed in these cases because of instability, irreproducibility, or low yield issues. In particular, the latter complex (isostructural to **1**), could only be observed in traces. In that respect, the easy and high yielding formation of stable crystals of **1** is remarkable. The synthetic strategy leading to complex **2**, with the hexafluorosilicate anions produced in situ, is highly effective but not particularly common in the literature. Subtle structural differences between **1**/**2** and the nitrate-containing literature examples (**5a**−**5c**) comprise the absence of coordinated counterions, shorter Cu···Cu separations through either the bpm or di-μ-hydroxo bridges and, more importantly, smaller Cu−OH−Cu θ angles, this latter justifying the stronger ferromagnetic coupling measured in **1** and **2** (see Table 2) with respect to **5a**−**5c**. Of note, the largest ferromagnetic coupling for this family of complexes (either dimers or chains) corresponds to that observed in **1** and **2**.

As part of this work, we set out to explore the possibility to substitute di-μ-hydroxo with di-μ-halo bridges, retaining the overall magnetic behavior. Synthetic attempts with X = Cl^- or Br^- only resulted in the formation of the previously reported 2D honeycomb complexes $[Cu_2(\mu\text{-bpm})X_4]$,[18a,b] regardless of the reaction conditions. The reaction between $Cu(NO_3)_2{\cdot}3H_2O$, bpm, and an organic fluoride salt (Bu_4NF) in alcohol media and plastic vessels produced, instead, a series of mono- (**4**) or dinuclear complexes,[32] as well a 1D polymer of the desired type, compound **3**. Complexes **3** and **4** represent the first bpm/F- complexes reported to date. Alternating μ-bpm and di-μ-fluoro bridges are present in **3**, exhibiting, however, a mutually orthogonal arrangement as opposed to the coplanar motif observed in the bpm/hydroxo chains **1** and **2**. The axial−equatorial coordination of the bpm at each copper(II) ion in a centrosymmetric manner vanishes practically; this exchange pathway in **3** and the weak antiferromagnetic coupling observed, substantiated also by theoretical calculations, are assigned to the di-μ-fluoro pathway.

■ ASSOCIATED CONTENT

Ⓢ Supporting Information

Crystallographic data in CIF format for **1**−**4**. This material is available free of charge via the Internet at http://pubs.acs.org.

■ AUTHOR INFORMATION

Corresponding Author

*Phone: (+39)-0984-49-2068 (G.D.M.), (+34)-96-354-44-40 (M.J.). E-mail: demunno@unical.it (G.D.M.), miguel.julve@uv.es (M.J.).

Present Address

[‖]Department of Chemistry, Syracuse University, Syracuse, NY 13244−4100, United States.

Notes

The authors declare no competing financial interest.

■ ACKNOWLEDGMENTS

This work was supported by the Italian Ministero dell'Istruzione, dell'Università e della Ricerca Scientifica through the Centro di Eccellenza CEMIF.CAL (Grant CLAB01TYEF) and the Ministerio de Educación y Ciencia (MEC, Spain) through Projects CTQ2010-15364) and Consolider Ingenio CSD-2007-00010 (Molecular Nanociencia). G.D.M. acknowledges the University of Valencia for a Visiting Professor fellowship.

■ REFERENCES

(1) Kahn, O. *Molecular Magnetism*; VCH: Weinheim, Germany, 1993.

(2) *Magnetism: A Supramolecular Function*; Kahn, O. Ed.; Kluwer: Dordrecht, The Netherlands, 1995; NATO ASI Ser. C, Vol. *484*.

(3) (a) *Magnetism: Molecules to Materials: Models and Experiments*; Miller, J. S., Drillon, M., Eds.; Wiley-VCH: Weinheim, Germany, 2001; Vol. *1*. (b) *Magnetism: Molecules to Materials II: Molecule Based Materials*; Miller, J. S., Drillon, M., Eds.; Wiley-VCH: Weinheim, Germany, 2001; Vol. *2*. (c) *Magnetism: Molecules to Materials III: Nanosized Magnetic Materials*; Miller, J. S., Drillon, M., Eds.; Wiley-VCH: Weinheim, Germany, 2002; Vol. 3. (d) *Magnetism: Molecules to Materials IV*; Miller, J. S., Drillon, M., Eds.; Wiley-VCH: Weinheim, Germany, 2003; Vol. *4*. (e) *Magnetism: Molecules to Materials V*; Miller, J. S., Drillon, M., Eds.; Wiley-VCH: Weinheim, Germany, 2005; Vol. *5*.

(4) *Molecular Magnets. Recent Highlights*; Linert, W., Verdaguer, M., Eds.; Springer-Verlag: Wien, Austria, 2003.

(5) Miller, J. S. *Chem. Soc. Rev.* **2011**, *40*, 3266.

(6) (a) Lescouëzec, R.; Toma, L. M.; Vaissermann, J.; Verdaguer, M.; Delgado, F. S.; Ruiz-Pérez, C.; Lloret, F.; Julve, M. *Coord. Chem. Rev.* **2005**, *249*, 2691. (b) Bogani, L.; Vindigni, A.; Sessoli, R.; Gatteschi, D. *J. Mater. Chem.* **2008**, *18*, 4750. (c) Miyasaka, H.; Julve, M.; Yamashita, M.; Clérac, R. *Inorg. Chem.* **2009**, *48*, 3420. (d) Coronado, E.; Galán-Mascarós, J. R.; Martí-Gastaldo, C. *CrystEngComm* **2009**, *11*, 2143. (e) Sun, H. L.; Wang, M.; Gao, S. *Coord. Chem. Rev.* **2010**, *254*, 1081. (f) Pardo, E.; Train, C.; Lescouëzec, R.; Journaux, Y.; Pasán, J.; Ruiz-Pérez, C.; Delgado, F. S.; Ruiz-García, R.; Lloret, F.; Paulsen, C. *Chem. Commun.* **2010**, *46*, 2322. (g) Liu, T.; Zhang, Y. J.; Kanegawa, S.; Sato, O. *J. Am. Chem. Soc.* **2010**, *132*, 8250.

(7) *Organic and Inorganic Low-Dimensional Crystalline Materials*; Delhaes, P., Drillon, M., Eds.; NATO AS1 Series 168; Plenum: New York, 1987.

(8) Chen, C.-T.; Suslick, K. S. *Coord. Chem. Rev.* **1993**, *128*, 293.

(9) (a) Viau, G.; Lombardi, M. G.; De Munno, G.; Julve, M.; Lloret, F.; Faus, J.; Caneschi, A.; Clemente-Juan, J. M. *Chem. Commun.* **1997**, 1195. (b) Cortés, R.; Drillon, M.; Solans, X.; Lezama, L.; Rojo, T. *Inorg. Chem.* **1997**, *36*, 677. (c) Abu-Youssef, M. A. M.; Escuer, A.; Gatteschi, D.; Goher, M. A. S.; Mautner, F. A.; Vicente, R. *Inorg. Chem.* **1999**, *38*, 5716. (d) Triki, S.; Thétiot, F.; Vandevelde, F.; Sala-Pala, J.; Gómez-García., C. J. *Inorg. Chem.* **2005**, *44*, 4086.

(10) (a) De Groot, H. J. M.; de Jongh, L. I.; Willett, R. D.; Reedijk. *J . Appl. Phys.* **1982**, *53*, 8038. (b) Benelli., C.; Gatteschi., D.; Carnezie., D. W.; Carlin., R. L. *J. Am. Chem. Soc.* **1985**, *107*, 2560. (c) Vasileveskv, I.; Rose, N. R.; Stenkamu, R.; Willett, R. D. *Inorg. Chem.* **1991**, *30*, 4082.

(11) Mixed OH/bpm Cu(II) complexes: (a) De Munno, G.; Julve, M.; Lloret, F.; Faus, J.; Verdaguer, M.; Caneschi, A. *Angew. Chem., Int. Ed. Engl.* **1993**, *32*, 1046. (b) De Munno, G.; Julve, M.; Lloret, F.; Faus, J.; Verdaguer, M.; Caneschi, A. *Inorg. Chem.* **1995**, *34*, 157. (c) Kirk, M. L.; Hatfield, W. E.; Lah, M. S.; Kessissoglou, D.; Pecoraro, V. L.; Morgan, L. W.; Petersen, J. D. *J. Appl. Phys.* **1991**, *69*, 6013.

(12) (a) De Munno, G.; Lombardi, M. G.; Julve, M.; Lloret, F.; Faus, J. *Inorg. Chim. Acta* **1998**, *282*, 82. (b) Escuer, A.; Font-Bardía, M.; Peñalba, E.; Solans, X.; Vicente, R. *Polyhedron* **1999**, *18*, 211. (c) Shen, H. Y.; Bu, W. M.; Gao, E. Q.; Liao, D. Z.; Jiang, Z. H.; Yan, S. P.; Wang, G. L. *Inorg. Chem.* **2000**, *39*, 396. (d) Monfort, M.; Resino, I.; Ribas, J.; Solans, X.; Font-Bardía, M.; Rabu, P.; Drillon, M. *Inorg. Chem.* **2000**, *39*, 2572. (e) Xie, Y.; Liu, Q.; Jiang, H.; Du, C.; Xu, X.; Yu, M.; Zhu, Y. *New J. Chem.* **2002**, *26*, 176. (f) Gao, E. Q.; Bai, S. Q.; Wang, C. F.; Yue, Y. F.; Yan, C. H. *Inorg. Chem.* **2003**, *42*, 8456. (g) Triki, S.; Gómez-García, C. J.; Ruiz, E.; Sala-Pala, J. *Inorg. Chem.* **2005**, *44*, 5501. (h) You, Y. S.; Hong, C. S.; Kim, K. M. *Polyhedron* **2005**, *24*, 249. (i) Adhikary, C.; Koner, S. *Coord. Chem. Rev.* **2010**, *254*, 2933.

(13) Examples of mixed cyanide/bpm complexes can be found in: (a) Toma, L. M.; Lescouëzec, R.; Toma, L. D.; Lloret, F.; Julve, M.; Vaissermann, J.; Andruh, M. *J. Chem. Soc., Dalton Trans.* **2002**, 3171. (b) Colacio, E.; Domínguez-Vera, J. M.; Lloret, F.; Sánchez, J. M. M.; Kivekas, R.; Rodríguez, A.; Sillanpäa, R. *Inorg. Chem.* **2003**, *42*, 4209. (c) Herrera, J. M.; Armentano, D.; De Munno, G.; Lloret, F.; Julve, M.; Verdaguer, M. *New J. Chem.* **2003**, *27*, 128. (d) Colacio, E.; Lloret, F.; Navarrete, M.; Romerosa, A.; Stoeckli-Evans, H.; Suárez-Varela, J. *New J. Chem.* **2005**, *29*, 1189. (e) Colacio, E.; Debdoubi, A.; Kivekas, R.; Rodríguez, A. *Eur. J. Inorg. Chem.* **2005**, 2860. (f) Podgajny, R.; Pinkowicz, D.; Korzeniak, T.; Nitek, W.; Rams, M.; Sieklucka, B. *Inorg. Chem.* **2007**, *46*, 10416. (g) Suárez-Varela, J.; Sakiyama, H.; Cano, J.; Colacio, E. *Dalton Trans.* **2007**, 249. (h) Visinescu, D.; Fabelo, O.; Ruiz-Pérez, C.; Lloret, F.; Julve, M. *CrystEngComm* **2010**, *12*, 2454.

(14) Examples of mixed azide/bpm complexes can be found in: (a) De Munno, G.; Real, J. A.; Julve, M.; Muñoz, M. C. *Inorg. Chim. Acta* **1993**, *211*, 227. (b) De Munno, G.; Julve, M.; Viau, G.; Lloret, F.; Faus, J.; Viterbo, D. *Angew. Chem., Int. Ed.* **1996**, *35*, 1807. (c) Cortés, R.; Lezama, L.; Pizarro, J. L.; Arriortua, M. I.; Rojo, T. *Angew. Chem., Int. Ed.* **1996**, *35*, 1810. (d) De Munno, G.; Poerio, T.; Viau, G.; Julve, M.; Lloret, F.; Journaux, Y.; Rivière, E. *Chem. Commun.* **1996**, 2587. (e) Cortés, R.; Urtiaga, M. K.; Lezama, L.; Pizarro, J. L.; Arriortua, M. I.; Rojo, T. *Inorg. Chem.* **1997**, *36*, 5016. (f) van Albada, G. A.; Smeets, W. J. J.; Spek, A. L.; Reedijk, J. *J. Chem. Cryst.* **1998**, *28*, 427.

(15) Examples of mixed cyanate/bpm complexes can be found in: (a) Julve, M.; Verdaguer, M.; De Munno, G.; Real, J. A.; Bruno, G. *Inorg. Chem.* **1993**, *32*, 795. (b) De Munno, G.; Poerio, T.; Julve, M.; Lloret, F.; Viau, G.; Caneschi, A. *J. Chem. Soc., Dalton Trans.* **1997**, 601. (c) Cortés, R.; Urtiaga, M. K.; Lezama, L.; Pizarro, J. L.; Arriortua, M. I.; Rojo, T. *Inorg. Chem.* **1997**, *36*, 5016.

(16) Examples of mixed thiocyanate/bpm complexes can be found in ref 15a as well as in: De Munno, G.; Bruno, G.; Nicolo, F.; Julve, M.; Real, J. A. *Acta Crystallogr., Sect. C: Cryst. Struct. Commun.* **1993**, *49*, 457.

(17) Examples of mixed oxalate/bpm complexes can be found in: (a) De Munno, G.; Julve, M.; Nicolò, F.; Lloret, F.; Faus, J.; Ruiz, R.; Sinn, E. *Angew. Chem., Int. Ed.* **1993**, *32*, 613. (b) De Munno, G.; Ruiz, R.; Lloret, F.; Faus, J.; Sessoli, R.; Julve, M. *Inorg. Chem.* **1995**, *34*, 408. (c) Decurtins, S.; Schmalle, H. W.; Schneuwly, P.; Zheng, L. M.; Ensling, J.; Hauser, A. *Inorg. Chem.* **1995**, *34*, 5501. (d) Armentano, D.; De Munno, G.; Lloret, F.; Julve, M.; Curély, J.; Babb, A. M.; Lu, J. Y. *New J. Chem.* **2003**, *27*, 161.

(18) Mixed Cl-Br/bpm Cu(II) complexes: (a) ref 17c. (b) Julve, M.; De Munno, G.; Bruno, G.; Verdaguer, M. *J. Chem. Res.* **1987**, 152. (c) Julve, M.; De Munno, G.; Bruno, G.; Verdaguer, M. *Inorg. Chem.* **1988**, *27*, 3160.

(19) (a) De Munno, G.; Julve, M.; Lloret, F.; Cano, J.; Caneschi, A. *Inorg. Chem.* **1995**, *34*, 2048. (b) Kawata, S.; Kitagawa, S.; Enomoto, M.; Kumagai, H.; Katada, M. *Inorg. Chim. Acta* **1998**, *283*, 80. (c) De Munno, G.; Poerio, T.; Julve, M.; Lloret, F.; Faus, J.; Caneschi, A. *J. Chem. Soc., Dalton Trans.* **1998**, 1679.

(20) (a) Hatfield, W. E. In *Magneto-Structural Correlations in Exchange Coupled Systems*; Willett, R. D., Gatteschi, D., Kahn, O., Eds.; NATO AS1 Series 140; Reidel: Dordrecht, The Netherlands, 1985; p 555 and references therein. (b) Crawford, V. H.; Richardson, H. W.; Wasson, J. R.; Hodgson, D. J.; Hatfield, W. E. *Inorg. Chem.* **1976**, *15*, 2107.

(21) Earnshaw, A. *Introduction to Magnetochemistry*; Academic Press: London, U.K., 1968.

(22) Becke, A. D. *J. Chem. Phys.* **1993**, *98*, 5648.

(23) *Jaguar 6.0*; Schrödinger, Inc.: Portland, OR, 2005.

(24) (a) Schafer, A.; Horn, H.; Ahlrichs, R. *J. Chem. Phys.* **1992**, *97*, 2571. (b) Schaefer, A.; Huber, C.; Ahlrichs, R. *J. Chem. Phys.* **1994**, *100*, 5829.

(25) (a) Ruiz, E.; Alemany, P.; Alvarez, S.; Cano, J. *J. Am. Chem. Soc.* **1997**, *119*, 1297. (b) Ruiz, E.; Cano, J.; Alvarez, S.; Alemany, P. *J. Comput. Chem.* **1999**, *20*, 1391. (c) Ruiz, E.; Rodríguez-Fortea, A.; Cano, J.; Alvarez, S.; Alemany, P. *J. Comput. Chem.* **2003**, *24*, 982. (d) Ruiz, E.; Alvarez, S.; Cano, J.; Polo, V. *J. Chem. Phys.* **2005**, *123*, 164110. (e) Ruiz, E.; Cano, J.; Alvarez, S.; Alemany, P. *J. Am. Chem. Soc.* **1998**, *120*, 11122. (f) Ruiz, E.; Cano, J.; Alvarez, S.; Caneschi, A.; Gatteschi, D. *J. Am. Chem. Soc.* **2003**, *125*, 6791.

(26) *SAINT*, Version 6.45; Bruker Analytical X-ray Systems Inc.: Madison, WI, 2003.

(27) *SADABS*, Version 2.03; Bruker AXS Inc.: Madison, WI, 2000.

(28) *SHELXTL NT*, Version 5.10; Bruker Analytical X-ray Inc.: Madison, WI, 1998.

(29) Nardelli, M. *J. Appl. Crystallogr.* **1995**, *28*, 659.

(30) *DIAMOND 3.1b*; Crystal Impact GbR, CRYSTAL IMPACT K; Brandeburg & H. Putz GBR: Bonn, Germany, 2006.

(31) Armentano, D.; De Munno, G., unpublished result.

(32) Marino, N. Ph.D. Thesis, University of Calabria, Cosenza, Italy, 2009.

(33) Castro, I.; Julve, M.; De Munno, G.; Bruno, G.; Real, J. A.; Lloret, F.; Faus, J. *J. Chem. Soc., Dalton Trans.* **1992**, 1739.

(34) For the in situ SiF_6^{2-} formation see, for instance: (a) Cotton, A.; Wilkinson, G. *Advanced Inorganic Chemistry*, 2nd ed.; Interscience Publishers : New York, 1966; p. 478; (b) Casellas, H.; Pevec, A.; Kozlevcar, B.; Gamez, P.; Reedijk, J. *Polyhedron* **2005**, *24*, 1549. (c) Mastropietro, T. F.; Armentano, D.; Grisolia, E.; Zanchini, C.; Julve, M.; Lloret, F.; De Munno, G. *Dalton Trans.* **2008**, 514.

(35) For the incorporation of F^- anions as consequence of the BF_4^- decomposition see, for instance: (a) Rietmeijer, F. J.; de Graaff, R. A. G.; Reedijk, J. *Inorg. Chem.* **1984**, *23*, 151 , and references therein. (b) Manzur, J.; Vega, A.; Garcia, A. M.; Acuna, C.; Sieger, M.; Sarkar, B.; Niemeyer, M.; Lissner, F.; Schleid, T.; Kaim, W. *Eur. J. Inorg. Chem.* **2007**, 5500.

(36) Nakamoto, K. *Infrared and Raman Spectra of Inorganic and Coordination Compounds, Part B, Applications in Coordination, Organometallics and Bioinorganic Chemistry*, 5th ed.; Wiley: Chichester, 1997.

(37) (a) Infantes, L.; Motherwell, S. *CrystEngComm* **2002**, *4*, 454. (b) Infantes, L.; Chisholm, J.; Motherwell, S. *CrystEngComm* **2003**, *5*, 480.

(38) Castro, I.; Sletten, J.; Glaerum, L. K.; Lloret, F.; Faus, J.; Julve, M. *J. Chem. Soc., Dalton Trans.* **1994**, 2777.

(39) Thetiot, F.; Triki, S.; Pala, J. S.; Galán-Mascaros, J.-R.; Martinez-Agudo, J. M.; Dunbar, K. R. *Eur. J. Inorg. Chem.* **2004**, 3783.

(40) (a) De Munno, G.; Bazzicalupi, C.; Faus, J.; Lloret, F.; Julve, M. *J. Chem. Soc., Dalton Trans.* **1994**, 1879. (b) Rodríguez-Martín, Y.; Sanchiz, J.; Ruiz-Pérez, C.; Lloret, F.; Julve, M. *Inorg. Chim. Acta* **2001**, *326*, 20.

(41) (a) De Munno, G.; Julve, M.; Verdaguer, M.; Bruno, G. *Inorg. Chem.* **1993**, *32*, 2215. (b) Castro, I.; Sletten, J.; Glaerum, L. K.; Cano, J.; Lloret, F.; Faus, J.; Julve, M. *J. Chem. Soc., Dalton Trans.* **1995**, 3207.

(42) (a) Rodríguez-Martín, Y.; Sanchiz, J.; Ruiz-Pérez, C.; Lloret, F.; Julve, M. *Inorg. Chim. Acta* **2001**, *326*, 20. (b) Vangdal, B.; Carranza, J.; Lloret, F.; Julve, M.; Sletten, J. *J. Chem. Soc., Dalton Trans.* **2002**, 566.

(43) (a) Borrás-Almenar, J. J.; Coronado, E.; Curély, J.; Georges, R.; Gianduzzo, J. J. *Inorg. Chem.* **1994**, *33*, 5171. (b) Borrás-Almenar, J. J. Ph.D. Thesis, University of València, València, Spain, 1992.
(44) (a) Girerd, J. J.; Charlot, M. F.; Kahn, O. *Mol. Phys.* **1977**, *34*, 1063. (b) Kahn, O.; Charlot, M. F. *New J. Chem.* **1980**, *4*, 567.
(45) (a) Duffy, W.; Barr, K. P. *Phys. Rev.* **1968**, *165*, 647. (b) Hall, J. W.; Marsh, W. E.; Weller, R. R.; Hatfield, W. E. *Inorg. Chem.* **1981**, *20*, 1033.
(46) Rietmeijer, F. J.; de Graaff, R. A. G.; Reedijk, J. *Inorg. Chem.* **1984**, *23*, 151.